Analysis of the Rice Mutant *dwarf and gladius leaf 1*. Aberrant Katanin-Mediated Microtubule Organization Causes Up-Regulation of Gibberellin Biosynthetic Genes Independently of Gibberellin Signaling

Masahiko Komorisono, Miyako Ueguchi-Tanaka, Ikuko Aichi, Yasuko Hasegawa, Motoyuki Ashikari, Hidemi Kitano, Makoto Matsuoka, and Takashi Sazuka*

Bioscience and Biotechnology Center, Nagoya University, Nagoya, Aichi 464–8601, Japan

Molecular genetic studies of plant dwarf mutants have indicated that gibberellin (GA) and brassinosteroid (BR) are two major factors that determine plant height; dwarf mutants that are caused by other defects are relatively rare, especially in monocot species. Here, we report a rice (*Oryza sativa*) dwarf mutant, *dwarf and gladius leaf 1* (*dgl1*), which exhibits only minimal response to GA and BR. In addition to the dwarf phenotype, *dgl1* produces leaves with abnormally rounded tip regions. Positional cloning of *DGL1* revealed that it encodes a 60-kD microtubule-severing katanin-like protein. The protein was found to be important in cell elongation and division, based on the observed cell phenotypes. GA biosynthetic genes are up-regulated in *dgl1*, but the expression of BR biosynthetic genes is not enhanced. The enhanced expression of GA biosynthetic genes in *dgl1* is not caused by inappropriate GA signaling because the expression of these genes was repressed by GA_3 treatment, and degradation of the rice DELLA protein SLR1 was triggered by GA_3 in this mutant. Instead, aberrant microtubule organization caused by the loss of the microtubule-severing function of DGL1 may result in enhanced expression of GA biosynthetic genes in that enhanced expression was also observed in a BR-deficient mutant with aberrant microtubule organization. These results suggest that the function of DGL1 is important for cell and organ elongation in rice, and aberrant DGL1-mediated microtubule organization causes up-regulation of gibberellin biosynthetic genes independently of gibberellin signaling.

Plant dwarfism is one of the most important phenotypes used in plant breeding, and more than 60 rice (*Oryza sativa*) dwarf mutants have been identified (Matsuo et al., 1997). Dwarfism arises from various types of defect, but two major factors responsible for dwarfism, gibberellin (GA) and brassinosteroid (BR), have been the most intensely studied. Numerous dwarf mutants are deficient in the biosynthesis or perception of these phytohormones (Mandava, 1988; Clouse and Sasse, 1998; Taiz and Zeiger, 2002; Fujioka and Yokota, 2003). For several years, our group has studied rice mutants defective in GA and BR biosynthesis or perception and cataloged the typical phenotypes of rice GA- and BR-related mutants. For example, rice GA-related mutants are typically dwarfs with deep green, rough leaves, but exhibit no other abnormal morphology (Sakamoto et al., 2004). In contrast, rice BR-deficient mutants are typically dwarfs with other abnormal morphologies, including malformed leaves with twisted, stiff blades (Hong et al., 2004).

In contrast to the extensive characterization of dwarf mutants related to GA and BR, dwarf mutants with phenotypes that differ from the typical GA- or BR-related phenotypes have not been well characterized. These uncharacterized dwarf mutants may be caused by various defects related to the elongation and/or division of stem cells. For example, analysis of the rice dwarf mutant *d3*, which exhibits dwarfism and increased tiller numbers, revealed that *D3* encodes an F-box Leu-rich-repeat protein orthologous to the Arabidopsis (*Arabidopsis thaliana*) MAX2/ORE9 (Ishikawa et al., 2005). This suggests that a novel F-box Leu-rich-repeat protein is involved in stem elongation in rice.

In an effort to further understand the molecular mechanisms of stem elongation in rice, we have collected dwarf mutants that show phenotypes that are different from the typical GA- or BR-related dwarf mutants. These mutants have been categorized into several groups according to their characteristics. For example, some mutants exhibit dwarfism with narrow leaves and increased tiller numbers; others show poor growth with erect, narrow leaves; and one dwarf group has leaves with a unique rounded tip. We further examined the latter group of dwarf mutants, *dwarf and gladius leaf 1* (*dgl1*), because these mutants also showed defects in root and flower elongation (see "Results"), suggesting that DGL1 may be involved in a fundamental mechanism in cell elongation in rice. The *DGL1* gene was found to encode a microtubule-severing katanin-like protein that is important in cell elongation and division in plants. We analyzed the relationship between DGL1 and GA and BR signaling

* Corresponding author; e-mail sazuka@agr.nagoya-u.ac.jp; fax 81–52–789–5226.

Article, publication date, and citation information can be found at www.plantphysiol.org/cgi/doi/10.1104/pp.105.062968.

and found that GA biosynthesis genes are up-regulated in *dgl1*, although the GA signaling is normal in this mutant. We discuss the possibility that the up-regulation of GA biosynthetic genes occurs due to aberrant microtubule organization, independently of GA feedback regulation, via GA signaling.

RESULTS

Characterization of the *dgl1* Mutant

The *dgl1* mutants show two characteristic phenotypes: dwarfism and abnormal leaf blade morphology (Fig. 1). We screened for these characteristics to isolate three alleles with different severities (*dgl1-1*, *dgl1-2*, and *dgl1-3*). The *dgl1* leaves were shorter and the edges of the leaf tips were more rounded than in wild-type leaves (Fig. 1, B and C). This mutant showed inhibited elongation of the seminal and crown roots and reduced numbers of crown roots (Fig. 1D). The development of *dgl1* floral organs was also impaired. The rice flower is composed of one pair of glumes, one lemma, one palea, two lodicules, six stamens, and two stigmas arranged from the peripheral to the central direction (Fig. 1F, far left). The *dgl1* flowers were stunted and the lemma and palea were rounded (Fig. 1E). The *dgl1* flowers also developed short anthers and filaments (Fig. 1G) and a short, shrunken stigma (Fig. 1H). The severity of each of these abnormal leaf and flower phenotypes correlated with the level of dwarfism. The fertility of the mutants, even those with relatively mild phenotypes, was significantly lower than that of the wild type. These observations indicate that the loss of function of the *DGL1* gene causes multiple pleiotropic defects in various organs.

We also examined the plastochron of the *dgl1* mutants (Table I). The plastochron of the severe mutant (*dgl1-3*) was longer than that of the wild type, although the heading times of these two plants were similar. Consequently, the leaf number of the mutant was lower than that of the wild type. This suggests the possibility that the cell proliferation rate of the mutant is reduced (see below).

Cell Morphology and Organization in *dgl1*

We suspected that the abnormal development of the leaves, roots, and flowers of *dgl1* was caused by a defect in cell elongation and/or division. We therefore investigated the microscopic structure of *dgl1*

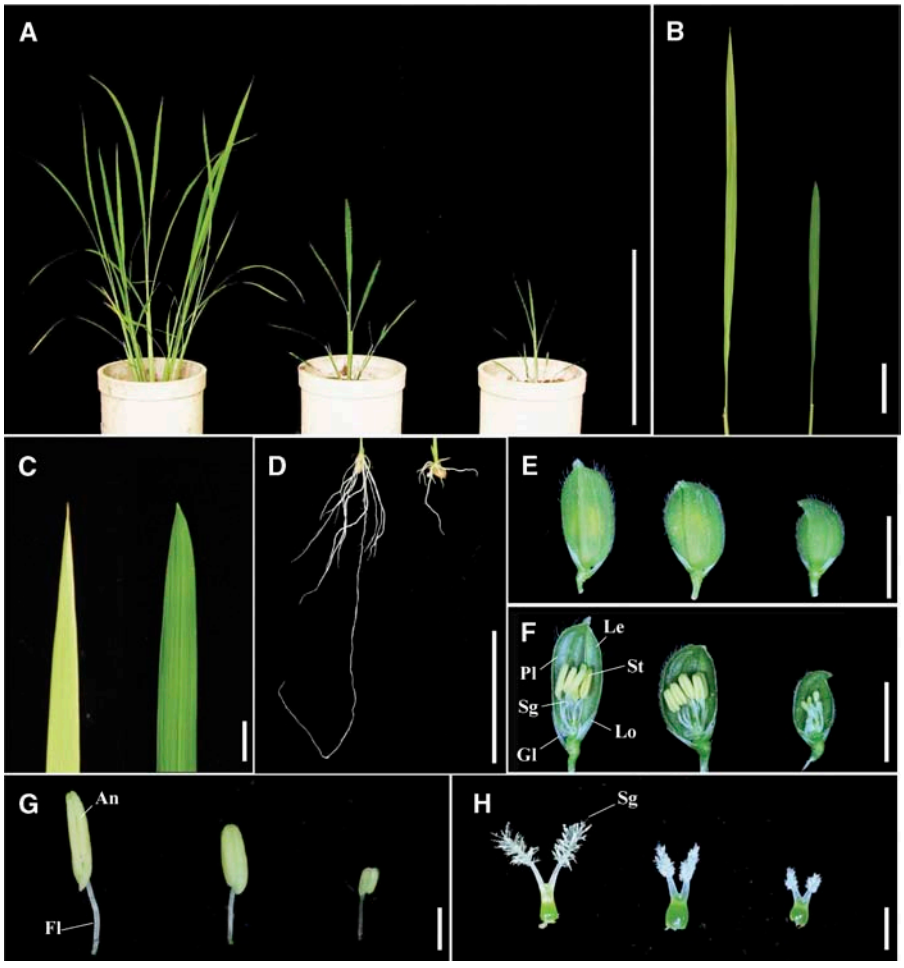

Figure 1. Morphological characteristics of the *dgl1* mutants. A, Gross morphology of *dgl1* at 1 month after sowing. From left to right, Wild type, *dgl1-2* (mild allele), and *dgl1-3* (strong allele). Bar = 30 cm. B, Leaf blade morphology of wild type (left) and *dgl1-3* (right). Bar = 5 cm. C, Leaf tip morphology of wild type (left) and *dgl1-3* (right). Bar = 1 cm. D, Root morphology of wild type (left) and *dgl1-3* (right). Bar = 5 cm. E, Morphology of flower exteriors. From left to right, Wild type, *dgl1-2*, and *dgl1-3*. Bar = 5 mm. F, Morphology of flower interiors. From left to right, Wild type, *dgl1-2*, and *dgl1-3*. Gl, Glume; Le, lemma; Pl, palea; Lo, lodicule; Sg, stigma; St, stamen. Bar = 5 mm. G, Stamens. From left to right, Wild type, *dgl1-2*, and *dgl1-3*. An, Anther; Fl, filament. Bar = 1 mm. H, Pistils. From left to right, Wild type, *dgl1-2*, and *dgl1-3*. Sg, Stigma. Bar = 1 mm.

Table I. *Plastochron and leaf numbers of wild-type and dgl1-3 plants* SD in parentheses; $n = 35$.

	Wild Type	*dgl1-3*
Plastochron days	6.2	8.7
Maximum leaf numbers	13.87 (0.52)	11.55 (0.69)

leaves. In wild-type plants, the elongated epidermal cells of the leaf blades were arranged in a longitudinal manner and formed well-organized cell files (Fig. 2A). In contrast, the longitudinally arranged cells of the mutant were not well elongated and the cells became bulky and distorted, leading to a disorganized cell file (Fig. 2, B and C). It is noteworthy that the shapes and sizes of the abnormal cells differed, with crescent-, triangle-, trapezoid-, or circular-shaped cells observed, in contrast to the wild type, which developed only rectangular cells (Fig. 2B, arrowheads). In the wild type, the stomatal cells alternated with ordinary epidermal cells to form a linear arrangement, but the equivalent line in *dgl1* was disturbed (Fig. 2, A and B, arrows). The elongated, narrow epidermal cells were arranged in a gentle curve at the tip of the wild-type leaf blade (Fig. 2D). In contrast, in *dgl1*, the epidermal cells at the tip of the leaf blade, in the abnormally

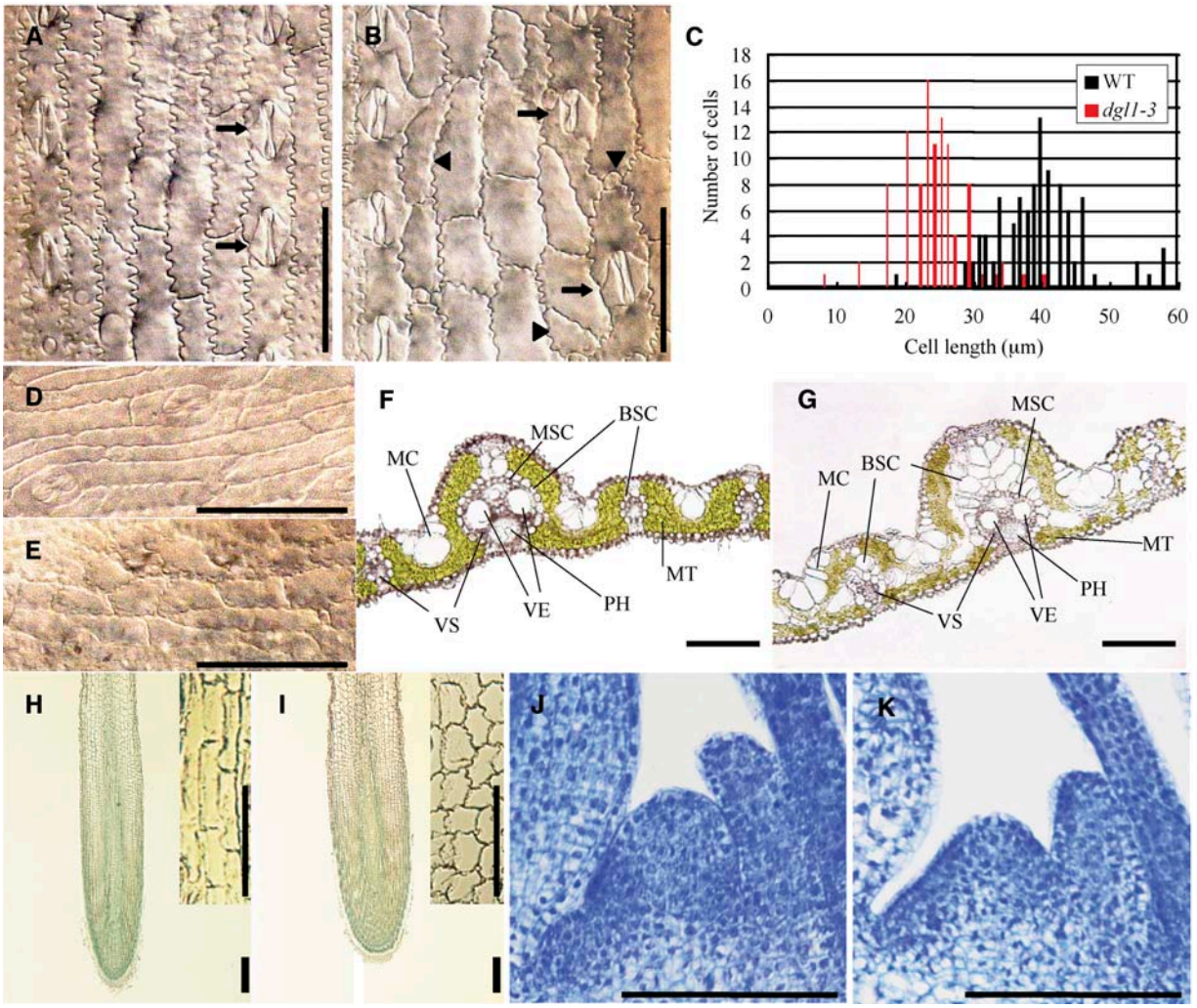

Figure 2. Structures of cells in various *dgl1* tissues. A and B, Epidermal cell morphology of wild-type and *dgl1-3* leaf blades, respectively. Arrows indicate stomatal cells. Cells with triangular, crescent, or round and small shapes are indicated in B by arrowheads. Bars = 50 μm. C, Distribution of the lengths of leaf blade surface cells of wild-type and *dgl1-3* plants. D and E, Epidermal cell morphology in the tip regions of wild-type and *dgl1-3* leaf blades, respectively. Bars = 50 μm. F and G, Cross sections of wild-type and *dgl1-3* leaf blades, respectively. In *dgl1*, the bundle sheath cells (BSC) are vacuolated and arranged in a disordered fashion in double or triple layers. The mother cells (MC) are also enlarged. VS, Vascular bundles; MSC, mestome sheath cells; VE, vessels; PH, phloem; MT, mesophyll tissue. Bars = 100 μm. H and I, Longitudinal sections of wild-type and *dgl1-3* roots stained with toluidine blue, respectively. Bars = 100 μm. Close-up views of the elongation zones are superimposed at the top right in each image. Bars = 50 μm. J and K, Longitudinal sections of the SAMs of wild-type and *dgl1-3* plants stained with toluidine blue, respectively. Bars = 100 μm.

rounded region, were not well elongated; additionally, the cell file was not well organized (Fig. 2E). These abnormal cell shapes and disorganized cell arrangements may be caused by a defect in synchronous division and elongation in these cells. In fact, the transverse division of cells in the mutant was often slanted, whereas this abnormal division pattern was not observed in the wild type.

We also observed the internal structure of wild-type and *dgl1* leaf blades using transverse sections. Figure 2, F and G, show cross sections of large vascular bundles in the wild type and *dgl1*, respectively. In the wild type, the large vascular bundle is located within the high ridge and the small vascular bundles are located within the low ridge (Fig. 2F). The valleys between the two ridges contain several motor cells. Mesophyll tissue is present between the vascular bundles. Each large and small vascular bundle is encircled by bundle sheath cells that contain a few chloroplasts with low chlorophyll content. Inside the bundle sheath cells, there are smaller cells also arranged in a ring, which forms the mestome sheath. The xylem is located on the upper side of the vascular bundles, and the two large vessels are well defined in the large vascular bundles. The phloem is located on the lower side of the vascular bundles. In the small vascular bundles, the vessels are thin and there are few phloem sieve tube elements.

The fundamental structure composed of the vascular bundles, motor cells, mesophyll tissues, and other tissues was present in *dgl1*, although the bundle sheath cells were enlarged and vacuolated (Fig. 2G). The single-layer structure of the bundle sheath cells was also disordered in *dgl1*, and the enlarged and vacuolated cells occurred in piles between the vascular and mesophyll cells. In contrast, decreased numbers of mesophyll cells were present in *dgl1* (Fig. 2G). The development of the small vascular bundles was also disturbed in the mutant, and the mutant contained increased numbers of motor cells (Fig. 2G).

The internal structure of the seminal root was also studied. In the wild type, cells of the elongation zone were well elongated and organized into cell files (Fig. 2H). In contrast, the elongation zone cells in *dgl1* were not elongated or well organized and were abnormally shaped (Fig. 2I). In the *dgl1* shoot apical meristem (SAM; Fig. 2, J and K), the size of the SAM dome was smaller than that of the wild type, probably because cell division might not proceed smoothly in *dgl1*, or cell size of the mutant is smaller than the wild type.

The *dgl1* Mutant Exhibits Only a Minimal Response to GA and BR

Phenotypic analyses of *dgl1* suggested that, in this mutant, cell division and elongation were ubiquitously inhibited. Because treatment with GA or BR rescues the dwarf phenotype of certain rice dwarf mutants, we treated the mutant with GA_3 or brassinolide (BL). As controls, the wild type, the GA-deficient *d35/Tan-Ginbozu* mutant (Itoh et al., 2004), and the *brd1-1* BR-deficient mutant (Hong et al., 2002) were also treated. Treatment of the third-leaf sheaths of these plants with GA_3 concentrations higher than 10^{-7} M triggered elongation of the wild-type and *d35* leaf sheaths, whereas no response was observed in the *dgl1* mutants *dgl1-2* and *dgl1-3* (Fig. 3A). Wild-type and *d35* leaf sheaths both elongated after treatment with 10^{-4} M GA_3, whereas the *dgl1* mutants did not respond to any GA_3 concentration.

Next, we treated the third-leaf sheaths of plants with various concentrations of BL. In the BR-deficient mutant *brd1-1*, leaf sheath elongation was triggered by treatment with 10^{-9} M BL. In contrast, wild-type plants did not respond to this BL concentration, probably because the wild type contains a sufficient amount of endogenous bioactive BR (Fig. 3B). The mutants did not respond to treatment with BL at any concentration. The lack of response of the *dgl1* mutants to exogenous GA or BR suggests that the abnormal phenotypes of

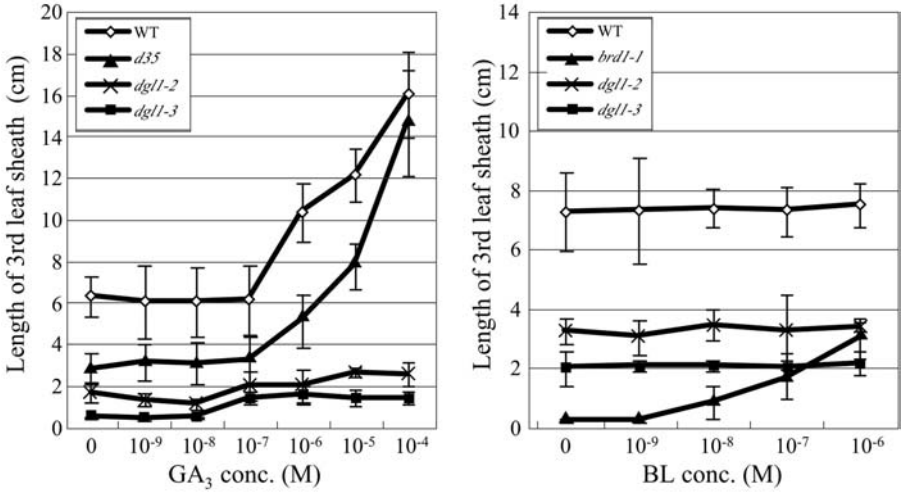

Figure 3. Elongation of the third-leaf sheath in response to GA_3 or BL treatment. The sheath length was measured at 3 d after treatment. Wild type, *d35* (GA-deficient mutant), and *brd1-1* (BR-deficient mutant) plants were used as controls. Error bars = the SD from the mean (n = 10).

the mutants are not caused by defects in GA or BR biosynthesis.

Positional Cloning of the *DGL1* Gene

Genetic analysis indicated that the *dgl1* mutation is recessive and is at a single locus (data not shown). We positionally cloned the *DGL1* gene to investigate the molecular nature of the encoded protein, using F_2 plants of a cross between *dgl1-1* (*japonica*) and Kasalath (*indica*). The F_2 plants segregated into two groups, with a 3:1 ratio of the normal and dwarf phenotypes. A total of 1,150 F_2 mutant plants were used for positional mapping of the *DGL1* locus. One derived cleaved amplified polymorphic sequence marker on chromosome 1, Cla3986, was found to be linked to the *dgl1-1* mutation (Fig. 4B). Fine mapping using several molecular markers designed around this position revealed that the *DGL1* locus is located in a 44.5-kb region between markers egr919-2 and Spe1624.

Five putative genes annotated by the Rice Genome Project are present in the 44.5-kb region. One of the genes was of special interest because it shows similarity to a 60-kD microtubule-associated ATPase katanin-like protein (KTN1). The loss of function of Arabidopsis *KTN1* causes a dwarf phenotype (Bouquin et al., 2003). The deduced amino acid sequence of the rice *DGL1* gene is highly similar, over almost the entire sequence, to those of all of the katanin proteins of known sequence in other organisms (Fig. 4A), including KTN1 (81% identity), which is encoded by *FRA2/BOT1/AtKSS/ERH3/LUE1* (Bichet et al., 2001; Burk et al., 2001; McClinton et al., 2001; Webb et al., 2002; Bouquin et al., 2003). We sequenced the *dgl1* genes of the three *dgl1* mutants. The two mild alleles contained 1-bp substitutions that generated a 1-amino acid substitution from Ala to Val in exon 4 in the putative ATP-binding domain (*dgl1-1*), and a 1-amino acid substitution from Asp to Asn in exon 7 in the C terminus (*dgl1-2*; Fig. 4B). The severe allele, *dgl1-3*, contained a large deletion (1,788 bp) between exons 3 and 6, which corresponds to the entire ATP-binding domain, suggesting that *dgl1-3* is a null mutant. These results indicate that *DGL1* encodes a rice katanin-like protein.

To confirm that the gene corresponds to the *dgl1* locus, we performed a complementation experiment. A 9.5-kb DNA fragment containing the entire *DGL1* sequence was introduced into *dgl1-3* by *Agrobacterium tumefaciens*-mediated transformation. The dwarf phenotype of *dgl1-3* was rescued in all the plants that were resistant to hygromycin, the selection marker used for transformation (Fig. 5). These results confirm that the *dgl1* phenotype is caused by the loss of function of a rice katanin-like protein.

Disorganized Cortical Microtubule Arrays in *dgl1* Cells

The cells of the Arabidopsis *fra2* mutant, which is defective in KTN1, show abnormal microtubule distribution (Burk et al., 2001; Burk and Ye, 2002). Therefore, we examined the microtubule organization in *dgl1* cells. Elongating wild-type internode cells exhibited well-organized cortical microtubules that formed parallel arrays (Fig. 6A). In contrast, in elongating *dgl1*

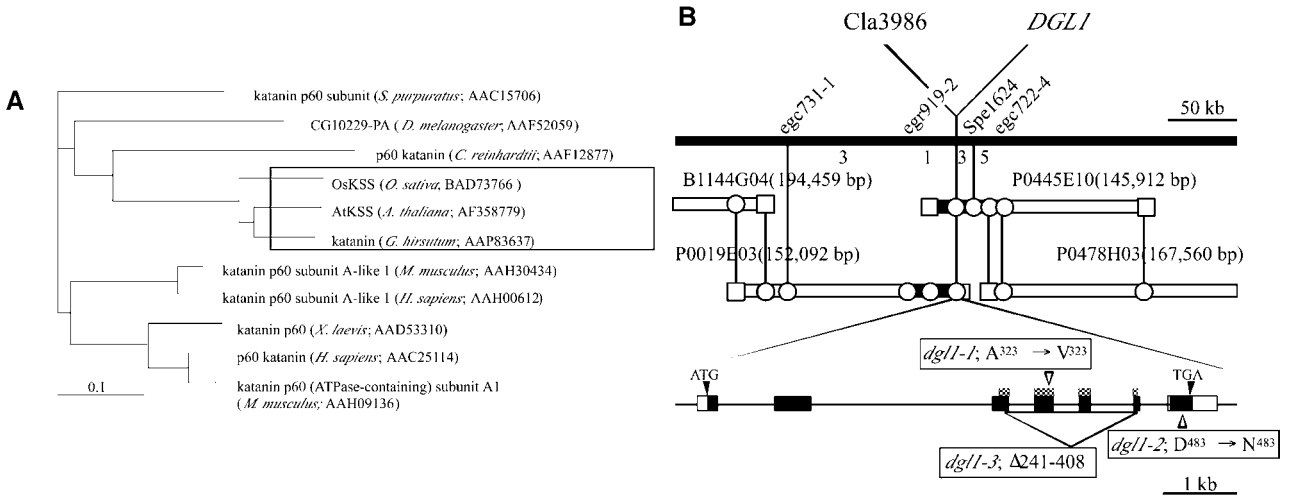

Figure 4. Phylogenic relationship between DGL1 and katanin-like proteins in other species and physical map of the *DGL1* gene. A, Phylogenetic relationship between DGL1 and katanin-like proteins in other organisms. The plant subgroup is boxed. The structural relationship was determined using ClustalW (http://www.ddbj.nig.ac.jp/search/clustalw-j.html) and illustrated using TreeView (http://taxonomy.zoology.gla.ac.uk/rod/treeview.html). B, High-resolution linkage and physical maps of the *DGL1* locus. The top line is a physical map around the *DGL1* locus of chromosome 1, near 121 cM. The vertical bars represent the molecular markers, and the numbers of recombinant plants are indicated between the markers. The *DGL1* mutation is tightly linked with the marker Cla3986. The *DGL1* gene consists of seven exons and six introns. Black and white boxes indicate the coding and noncoding regions in exons, and ATG and TGA indicate the sites of translation initiation and stop, respectively. The mutations identified in *dgl1-1*, *dgl1-2*, and *dgl1-3* are indicated. Checkered boxes indicate the ATP-binding domain.

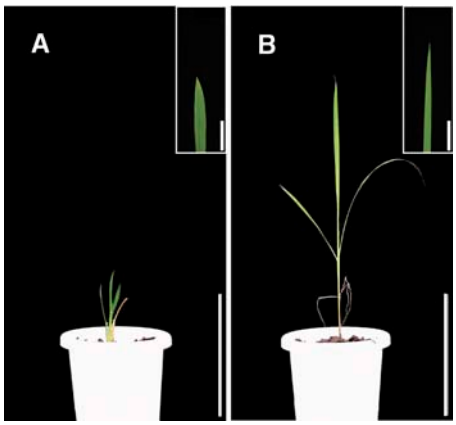

Figure 5. Phenotypic complementation by the introduction of *DGL1*. A, Regenerated *dgl1-3* plant transformed with the empty vector. Bar = 15 cm. B, A *dgl1-3* plant transformed with a DNA fragment encompassing the entire *DGL1* gene. Bar = 15 cm. The images superimposed at the top right are close-up views of the tip of leaf blade. Bar = 5 cm.

internode cells, the cortical microtubules were disorganized and arranged obliquely instead of in a parallel manner (Fig. 6B). This observation suggests that the *dgl1* mutation disrupts the function of the microtubule-severing katanin-like protein, resulting in the dwarf phenotype and other abnormal morphologies, because of the aberrant organization of cortical microtubules. The observation that KTN1 has in vitro microtubule-severing activity (Stoppin-Mellet et al., 2002) supports this idea (see below).

DGL1 Expression Analysis

The pleiotropic effect of the *dgl1* mutation in various organs indicates that the *DGL1* gene functions in all of these organs. Therefore, we examined the expression of *DGL1* in various rice organs with RNA gel-blot analysis using, as a probe, the entire length of the 3′-untranslated region of its cDNA. As expected, hybridizing bands were observed in RNAs extracted from each of the organs (Fig. 7A). RNAs extracted from the elongating stem and the SAM produced the strongest bands, and a band of intermediate intensity was produced using RNA from flowers, whereas RNAs from expanded leaf blades and sheaths and elongated roots produced relatively low-intensity bands. The preferential expression of *DGL1* in the stems and the SAM, and the low expression in expanded leaves and elongated roots, may correspond to normal levels of cell division and/or elongation in these organs.

The steady-state level of the *DGL1* mRNA was studied in various GA-related mutants (Fig. 7B), as it has been reported that the GA level positively regulates *KTN1* expression (Bouquin et al., 2003). We used one GA-deficient mutant that shows a severe dwarf phenotype caused by a defect in the kaurenoic acid oxidase (KAO) activity, *oskao-3* (Sakamoto et al., 2004), as well as the GA-signaling-related mutants *gid2*, which shows a GA-insensitive dwarf phenotype caused by a defect in the GID2/F-box protein (Sasaki et al., 2003), and *slr1*, which shows a constitutive-GA-response slender phenotype caused by a defect in the SLR1/DELLA protein (Ikeda et al., 2001; Itoh et al., 2002). In these GA-related mutants, *DGL1* expression was very similar to that in the wild type (Fig. 7B), demonstrating that the transcriptional expression of *DGL1* is not regulated by GA signaling.

In the BR-deficient mutant *brd1* and in *dgl1*, an internal deletion allele, *DGL1*, was expressed at levels similar to those in the wild type (Fig. 7B). Therefore, BR does not regulate the expression of *DGL1*. Bouquin et al. (2003) discussed the possibility that KTN1 is involved in a feed-forward regulation of the transcription of its own gene, based on the markedly reduced *KTN1* mRNA levels in the KTN1 mutant *lue1*. The similar levels of *DGL1* mRNA in the wild type and *dgl1-3* demonstrate that *DGL1* expression is not regulated by the functioning of DGL1, at least in rice.

To confirm the lack of involvement of GA in *DGL1* expression, we also examined the expression of the gene in GA-treated seedlings of the GA-deficient mutant *oskao-3* (Fig. 7C). The levels of *DGL1* expression were similar before and after GA_3 treatment, whereas the *OsGA20ox2/SD1* gene, which is negatively regulated by GA, was down-regulated by GA_3. This result clearly shows that *DGL1* expression is independent of GA.

GA Signaling in *dgl1*

As mentioned above, *dgl1* plants showed almost no response to GA_3 (Fig. 3). Bouquin et al. (2003) reported that the loss of katanin function results in inappropriate feedback regulation of the GA biosynthetic

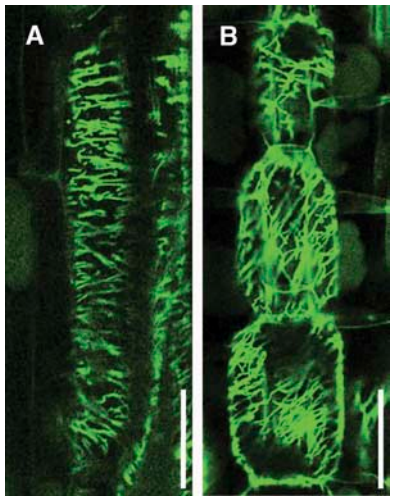

Figure 6. Arrangement of cortical microtubules in elongating internodal parenchyma cells. Internodal parenchyma cells were subjected to immunofluorescent staining for α-tubulin. The elongating cells in the wild type (A) contain transversely oriented cortical microtubules, whereas *dgl1-3* cells (B) contain aberrantly oriented cortical microtubules. Bars = 100 μm.

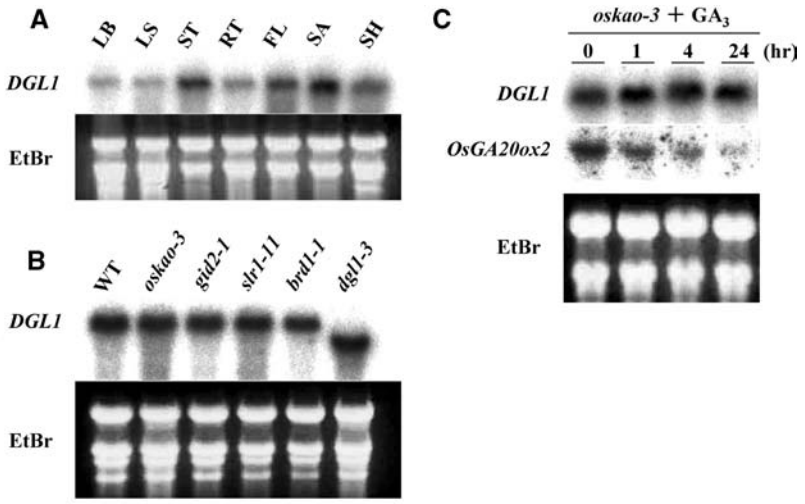

Figure 7. Expression of *DGL1*. A, Expression of *DGL1* in various organs of wild-type rice. Total RNA was isolated from leaf blade (LB), leaf sheath (LS), stem (ST), root (RT), young flower before heading (FL), shoot apex (SA), and entire young seedlings (SH). Five micrograms of total RNA were loaded in each lane. The gel was stained with ethidium bromide (EtBr) as a control. B, Expression of *DGL1* in GA- and BR-related mutants. Total RNAs were extracted from 1-month-old seedlings of the mutants and the RNAs were analyzed as in A. *oskao-3*, Severe-GA-deficient dwarf mutant; *gid2-1*, severe-GA-insensitive dwarf mutant; *slr1-11*, constitutive-GA-response slender mutant; *brd1-1*, severe-BR-deficient dwarf mutant; *dgl1-3*, severe allele of *dgl1*. C, *DGL1* expression in the GA-deficient mutant *oskao-3* after GA_3 treatment. The experiments were performed as in A. The expression of *OsGA20ox2/SD1* was also examined as a control for the GA_3 treatment. The down-regulation of *OsGA20ox2/SD1* indicates the functioning of the negative feedback regulation of GA signaling.

AtGA20ox1 gene, as well as partial GA insensitivity. Therefore, we investigated whether GA signaling is defective in *dgl1*. Using quantitative reverse transcription (RT)-PCR, we first examined the expression of three rice genes involved in GA biosynthesis, *OsGA20ox2/SD1*, *OsGA20ox1*, and *OsGA3ox2/D18*, the expression of all of which is negatively regulated by the level of GA in a feedback manner (Itoh et al., 2001, 2002). As expected, the expression of each of these genes was negatively regulated by GA treatment in the wild type in a feedback manner through the GA-signaling pathway (Fig. 8, A–C). In the *dgl1* mutants, the levels of *OsGA20ox2/SD1*, *OsGA20ox1*, and *OsGA3ox2/D18* transcripts were increased relative to those in the wild type, with the levels correlated to the severity of each allele (Fig. 8, A–C). In the severe allele *dgl1-3*, the levels of these transcripts were 2 or more times those in the wild type. In each of the *dgl1* alleles, the increased expression of these genes was suppressed by application of GA_3. The down-regulation of the GA biosynthetic genes in *dgl1* by GA_3 treatment indicates that the normal feedback regulation of these genes occurs in the *dgl1* mutants, despite their increased expression in the mutants.

These results suggested that the increased expression of these GA biosynthetic genes is due to a mechanism other than a defect in GA signaling. To examine this possibility, we examined the expression of GA biosynthetic genes for which the expression is not regulated by the GA level or GA signaling. Interestingly, the expression of the *OsKAO* gene, the product of which catalyzes the oxidation of *ent*-kaurenoic acid, was increased about 4 times in the mutants, as compared to the wild type, whereas GA_3 treatment did not affect the expression of this gene in wild-type or mutant plants (Fig. 8D). This observation demonstrates that the increased expression of the GA biosynthetic genes is not limited to genes regulated by GA signaling but that it also occurs in genes that are not affected by GA and suggests, consequently, that the increased expression of GA biosynthetic genes in *dgl1* is not related to GA signaling but is due, instead, to an unknown mechanism. We examined the expression of another GA biosynthetic gene, *OsKO2*, the product of which catalyzes the oxidation of *ent*-kaurene, and found that its expression in *dgl1* was very similar to that in the wild type (data not shown), indicating that not all GA biosynthetic genes are up-regulated in *dgl1*.

To confirm that normal GA signaling takes place in *dgl1*, we also examined the degradation of the SLR1 protein in the mutant using immunoblot analysis. SLR1, the sole DELLA protein in rice, functions as a repressor of GA signaling (Ikeda et al., 2001; Itoh et al., 2002; Fleet and Sun, 2005). The degradation of SLR1 is triggered by GA and is essential for the downstream action of GA (Sasaki et al., 2003). As previously reported, the GA-dependent degradation of SLR1 triggered by GA_3 occurred within 1 h in both wild-type and *dgl1-3* plants (Fig. 9, lanes 1–4), whereas no degradation was observed in the GA-insensitive mutant *gid2* (lanes 5 and 6). Furthermore, the level of SLR1 protein was similar in wild-type and *dgl1* plants not treated with GA_3, but was high in *gid2* (lanes 1, 3, and 5). The GA-dependent degradation of SLR1 and the similar levels

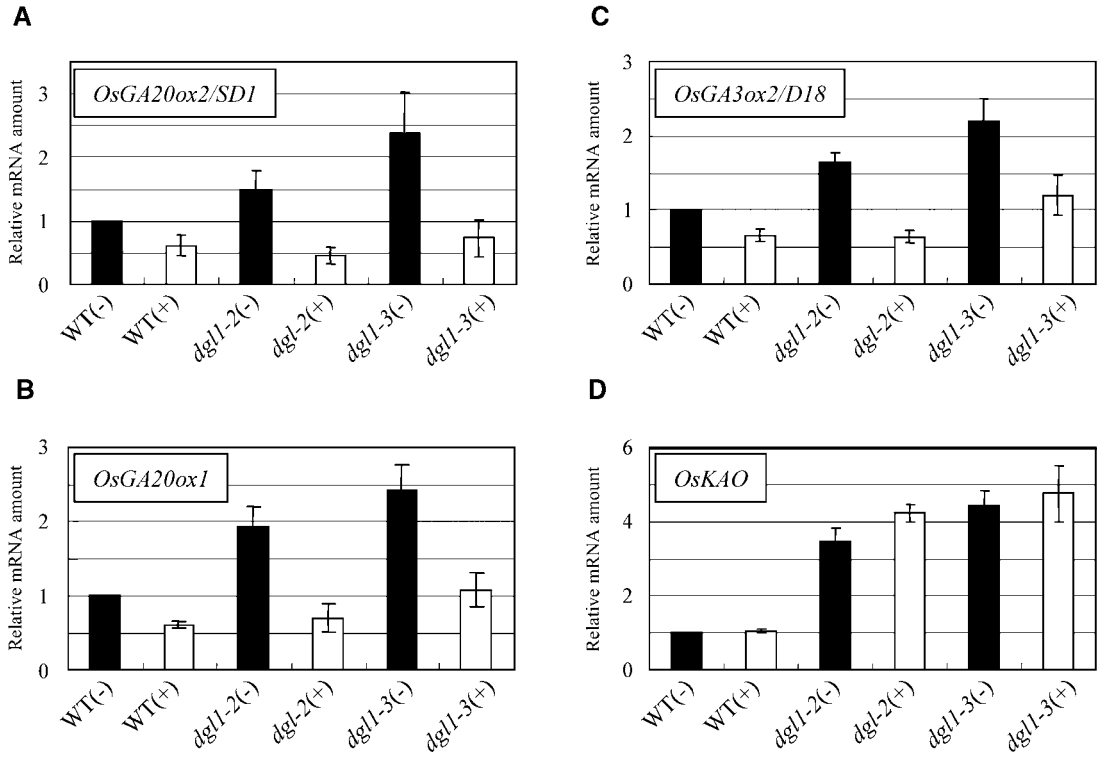

Figure 8. Enhanced expression of GA biosynthetic genes in *dgl1* and suppression by GA_3 treatment. Quantitative RT-PCR was performed using primers specific for each GA biosynthetic gene (see "Materials and Methods"). The plants were treated with (+) 10^{-4} M GA_3 or control solution (−). The expression of *OsGA20ox2/SD1* (A), *OsGA20ox1* (B), and *OsGA3ox2/D18* (C) was enhanced in *dgl1* and suppressed by GA_3 treatment, whereas *OsKAO* expression (D) was enhanced in *dgl1* but not suppressed by GA.

of the protein in wild-type and *dgl1* plants confirm that normal GA signaling takes place in *dgl1*.

The up-regulation of GA biosynthetic genes in *dgl1* suggested that BR biosynthetic genes are also up-regulated in the mutant. However, increased expression of BR biosynthetic genes was not observed in the mutants, including the genes corresponding to OsCPD (a homolog of the Arabidopsis CPD), D11 (Tanabe et al., 2005), and OsDWARF (a BR-C6 oxidase; Hong et al., 2002; data not shown). These observations indicate that, in contrast to GA biosynthesis, BR biosynthesis is not activated in the mutants.

Increased GA Biosynthetic Gene Expression Also Occurs in the BR-Deficient Mutant *brd1*

In both rice and Arabidopsis mutants defective in KTN1, GA biosynthetic genes are up-regulated. We questioned whether the lack of KTN1 activity or aberrant microtubule organization caused the up-regulation of these genes. Therefore, we measured the levels of the *OsGA20ox2/SD1*, *OsGA20ox1*, *OsGA3ox2/D18*, and *KAO* transcripts in the BR-deficient mutant *brd1-2*, in which the microtubule organization is thought to be aberrant (Yamamuro et al., 2000; Hong et al., 2002). The levels of transcripts of these genes in *brd1-2* were higher than in the wild type, and the high expression was suppressed by BL treatment (Fig. 10). These results strongly suggest that the up-regulation of these GA biosynthetic genes is caused by aberrant microtubule organization and is not a direct effect of the loss of KTN1 activity (see "Discussion").

DISCUSSION

DGL1 Encodes a Rice KTN1 Protein

The positional cloning of the *dgl1* locus revealed that *DGL1* encodes a rice KTN1, a 60-kD microtubule-associated ATPase katanin-like protein. Katanin is a microtubule-severing protein that disassembles microtubules into tubulin subunits while hydrolyzing ATP (Vale, 1991; McNally and Vale, 1993; McNally et al., 1996; Hartman et al., 1998; McNally and Thomas, 1998; Hartman and Vale, 1999). Katanin is a major microtubule-severing factor in animal cells and its activity was first identified in *Xenopus laevis* mitotic egg extracts (Vale, 1991). In sea urchin oocytes, katanin forms a heterodimer composed of 60- and 80-kD subunits that are a catalytic protein and a regulatory protein, respectively. The 60-kD subunit is a member of the AAA (ATPases associated with various cellular activities) protein family, and the animal katanin 80-kD subunit contains WD40 repeats. A recent model

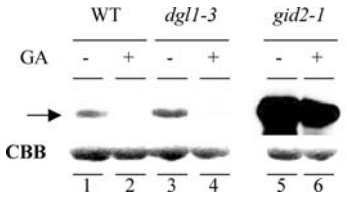

Figure 9. Degradation of SLR1 triggered by GA_3 treatment of *dgl1*. Protein gel-blot analysis of SLR1 in young seedlings of the wild type, *dgl1-3*, and the GA-insensitive mutant *gid2-1*. The plants were treated with (+) 10^{-4} M GA_3 or control solution (−), as described in "Materials and Methods." The arrow indicates the protein bands corresponding to endogenous SLR1. Each lane contains 10 μg of total protein. The loading control of Coomassie Brilliant Blue staining is shown.

proposes that the dimerization of these subunits is transient, and a ring-shaped p60 hexamer binds to and severs microtubules (Wasteneys, 2002). The hydrolysis of ATP by the 60-kD subunit is sufficient to sever microtubules in vitro (McNally et al., 2000), and the 80-kD subunit is involved in targeting the enzyme to the centrosome (Hartman et al., 1998). Thus, DGL1 may also sever microtubules in vivo.

Recently, a plant katanin-like protein was identified through analyses of Arabidopsis mutants. The inflorescence stems of the *fragile fiber 2* (*fra2*) mutant of Arabidopsis contain interfascicular fibers with defective mechanical strength (Burk and Ye, 2002). The *fra2* mutation causes a remarkable reduction in cell length and an increase in cell width in all organs, resulting in a global alteration in the morphology of the plant. The *FRA2* gene encodes KTN1. Recombinant KTN1 interacts with microtubules in cosedimentation assays and severs microtubules in vitro in the presence of ATP (Burk and Ye, 2002; Stoppin-Mellet et al., 2002). These results demonstrate that the plant KTN1 functions similarly to the animal katanin. The strong similarity of the primary structures of DGL1 and KTN1, as well as the phenotypic resemblance of *dgl1* and *fra2*, suggests that DGL1 has a function similar to that of KTN1. *dgl1* exhibited an unorganized cortical microtubule arrangement in elongating internodal parenchyma (Fig. 6). Burk and Ye (2002) proposed that the aberrant microtubule orientation caused by the mutation in KTN1 results in an altered deposition of cellulose microfibrils that leads to defective cell elongation. As defective cell elongation and aberrant microtubule orientation were observed in the rice *dgl1* mutants, the above model may explain the abnormal phenotype of *dgl1*, including its abnormal morphology, impaired root elongation, and stunted flowers.

We also found that the plastochron of the mutant (*dgl1-3*) is longer than that of the wild type (Table I), even though the size of the SAM in *dgl1* was smaller than that of the wild type (Fig. 2, J and K). The longer plastochron and smaller SAM indicate that the possibility that the mutant SAM exhibits reduced cell division frequency is not excluded and, therefore, that DGL1 activity may be involved not only in cell elongation but also in cell division. It is possible that the dwarf phenotype of *dgl1* is caused by disturbances in both cell elongation and cell division.

The Up-Regulation of GA Biosynthetic Genes in *dgl1* Is Not Caused by Inadequate GA Signaling But by Aberrant Cortical Microtubule Arrangement

Mundy and colleagues have reported that *AtGA20ox1/GA5*, the expression of which is negatively regulated by bioactive GA in a feedback manner, is upregulated in the KTN1-defective mutant *lue1*, and its expression in the mutant is further increased by GA_3 (Meier et al., 2001; Bouquin et al., 2003). This observation indicates that the loss of KTN1 function results in inappropriate feedback regulation of *AtGA20ox1/GA5* expression by GA, consequently inducing GA insensitivity. They also showed that the *KTN1* mRNA level is positively regulated by the level of GA (Bouquin et al., 2003). These observations suggested that microtubules and/or KTN1 activity are involved in the feedback control of GA synthesis, and that the GA-dependent modulation of the functioning of KTN1 might affect microtubule organization (Foster et al., 2003).

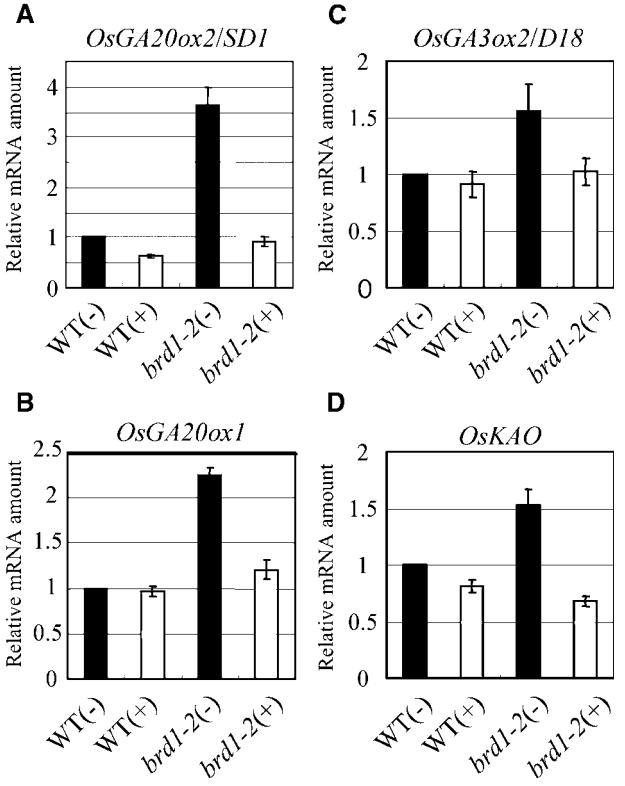

Figure 10. Enhanced expression of GA biosynthetic genes in the BR-deficient mutant *brd1-2* and suppression by BL treatment. Quantitative RT-PCR was performed using primers specific for each GA biosynthetic gene, as described in "Materials and Methods." Plants were treated with (+) 10^{-6} M BL or control solution (−), as described in "Materials and Methods." The expression levels of *OsGA20ox2/SD1* (A), *OsGA20ox1* (B), *OsGA3ox2/D18* (C), and *OsKAO* (D) were enhanced in *brd1-2* and suppressed by BL treatment.

We examined the possibility that this model applies to the *dgl1* mutant. In *dgl1* plants, as in *lue1* plants, certain GA biosynthetic genes, such as *OsGA20ox2/SD1*, *OsGA20ox1*, and *OsGA3ox2/D18*, are up-regulated. However, the up-regulation of these GA biosynthetic genes in *dgl1* may not be caused by inadequate feedback regulation of the genes because the increased levels of *OsGA20ox2/SD1*, *OsGA20ox1*, and *OsGA3ox2/D18* mRNAs that are normally observed in this mutant were prevented by GA_3 treatment, and the degradation of the rice DELLA protein SLR1 was triggered by GA. Moreover, a GA biosynthetic gene, *OsKAO*, whose expression is independent of the level of GA, is also up-regulated in *dgl1*. These observations indicate that the loss of DGL1 activity does not diminish GA signaling in rice.

Furthermore, the expression of the rice *DGL1* gene was found not to be regulated by GA (Fig. 7). Taken together, these results suggest that the aberrant arrangement of microtubules does not affect GA signaling, and GA does not affect *DGL1* expression, at least in rice. However, the aberrant microtubule organization may be related to the GA biosynthesis activity. In fact, up-regulation of GA biosynthetic genes was observed in both rice and Arabidopsis *KTN1* mutants. Interestingly, up-regulation of GA biosynthetic genes is not specific to DGL1-deficient mutants but is also observed in the BR-deficient mutant *brd1* (Fig. 10). This suggests that the loss of DGL1 function does not directly cause the enhanced GA biosynthetic gene expression. It is noteworthy that the aberrant microtubule organization does not enhance the expression of BR biosynthetic genes in contrast to GA biosynthetic genes. This suggests that an unknown specific mechanism connects the aberrant microtubule organization and the expression of the GA biosynthetic genes. Further studies will be necessary to reveal this mechanism.

MATERIALS AND METHODS

Plant Materials and Growth Conditions

Three *dgl1* mutant lines derived from rice (*Oryza sativa*), *dgl1-1*, *dgl1-2*, and *dgl1-3*, were used in this study. The *dgl1-1* and *dgl1-2* alleles were identified in a mutant library generated using *N*-methyl-*N*-nitrosourea. The *dgl1-3* allele, which was kindly donated by Dr. Hirochika (National Institute of Agrobiological Sciences, Tsukuba, Ibaraki, Japan), was derived from a rice plant (cv Nipponbare) regenerated from a cell suspension that had been in culture for several months. Wild-type rice plants, four *dgl1* alleles, the GA-deficient mutant *oskao-3*, the GA-insensitive mutant *gid2-2*, the constitutive-GA-response mutant *slr1-11*, and the BR-deficient mutant *brd1-1* were grown in a greenhouse at 30°C (day) and 24°C (night).

GA and BR Induction in Shoot Elongation

Seeds of wild-type and mutant rice lines were sterilized with 2.5% NaClO for 30 min and washed five times in sterile distilled water. The seeds were then placed on 1% agar plates, grown under fluorescent light at 30°C for 4 d, and then transferred to 1% agar plates containing various concentrations of GA_3 or BL. The length of the third-leaf sheath was measured at 4 d after application of GA_3 or 2 weeks after application of BL.

Mapping, Isolation, and Sequencing of *DGL1*

To map *DGL1*, F_2 plants from a cross between *dgl1-1* and the *indica* strain Kasalath were used. Approximately 1,150 F_2 plants of this cross were used for the positional cloning of *DGL1*. To identify the mutation sites in the *dgl1* alleles, *DGL1* was amplified using genomic DNA extracted from the three alleles. The amplified DNA fragments were sequenced directly using appropriate primers. A *DGL1* genomic DNA fragment was isolated from the PAC clone P0019E03, which is derived from the DNA bank of the Ministry of Agriculture, Forestry and Fisheries GenBank project. The clone contains the entire coding region and the 5′- and 3′-flanking regions of *DGL1*.

Complementation of the *dgl1* Mutant

A construct containing the *DGL1* gene was introduced into *dgl1-3*. The *DGL1* gene in the PAC clone P0019E03 (provided by the National Institute of Agrobiological Sciences) was digested with *Nae*I and *Bam*HI and inserted into the blunted *Xba*I site of a pBluescript vector. The clone was redigested with *Bam*HI and *Nae*I, after which the ends were filled in. The fragment of approximately 9.5 kb was fused into the *Sma*I site of the binary vector pBI-Hm12, which contains a hygromycin-resistance gene, kindly provided by Dr. Hiroyuki Hirano (Tokyo University, Tokyo). The binary vector was introduced into *Agrobacterium tumefaciens* strain EHA101 (Hood et al. 1986) by electroporation, and rice plants were transformed with this strain as described by Hiei et al. (1994). Control plants were generated by introducing the empty vector into *dgl1-3* mutant callus.

RNA Isolation and RNA Gel-Blot Analysis

Total RNAs (5 μg) isolated from various rice tissues using the RNeasy kit (Qiagen, Hilden, Germany) with the addition of an RNase-free DNase I treatment (TaKaRa Shuzo, Tokyo), and from seedlings of wild-type, *oskao-3*, *gid2-1*, *slr1-11*, *brd1-1*, and *dgl1-3* using the aurintricarboxylic acid method (Gonzalez et al. 1980), were separated on a 1% agarose gel and transferred to Hybond N^+ membrane (Amersham-Pharmacia, Piscataway, NJ). The membrane was hybridized with a ^{32}P-labeled partial *DGL1* cDNA fragment of 560 bp, which was amplified using the primers 5′-TGAAGTTGCACGGAGGACAG-3′ and 5′-CCAGCTTCCATGTTTCGCAC-3′, which correspond to regions in exon 7 and the 3′-untranslated region, respectively. To investigate the effects of GA_3 on *DGL1* expression, *oskao-3* seeds were grown on 1% agar plates under fluorescent light at 30°C for 7 d, sprayed with 10^{-4} M GA_3, and then harvested after 1 or 4 h. Total RNAs were isolated using the aurintricarboxylic acid method. Five and 10 μg of total RNAs were electrophoresed on 1% agarose gels and then transferred to membranes. An *OsGA20ox2*-specific probe of 420 bp was amplified from the cDNA and fused into pCRII (Invitrogen, Carlsbad, CA), and the resulting plasmid was digested with *Eco*RI. A *DGL1*-specific probe was prepared as described above. The membrane was hybridized at 65°C in a hybridization solution of 5× SSC (1× SSC = 0.15 M NaCl and 0.015 M sodium citrate), 5× Denhardt's solution (1× Denhardt's solution = 0.02% Ficoll, 0.02% polyvinylpyrrolidone, and 0.02% bovine serum albumin), 0.5% SDS, 10% dextran sulfate, and 0.1 mg mL^{-1} denatured salmon sperm DNA. DNA probes were labeled with ^{32}P-dCTP. The membrane was washed twice with 2× SSC and 0.1% SDS at 65°C for 20 min and once with 0.2× SSC and 0.1% SDS at 65°C for 10 min. The membranes were exposed to a Fuji imaging plate and the image was visualized using a BAS2000 imaging analyzer (Fuji Photo Film, Tokyo).

Observation of Microtubule Arrangement

Internodal parenchyma tissue was prefixed for 45 min at room temperature in 3.7% (w/v) paraformaldehyde in microtubule-stabilizing buffer (0.1 M piperazine-diethanolsulfonic acid, 1 mM $MgCl_2$, 5 mM EGTA, 0.2% (v/v) Triton X-100, 1% (w/v) glycerol, pH 6.9). Longitudinal sections were cut with a fresh razor blade, incubated in the above buffer for 40 min, and washed in microtubule-stabilizing buffer. The sections were then incubated for 1 h at 37°C with an α-tubulin rabbit monoclonal antibody (kindly donated by Dr. Mizuno, Osaka University, Osaka) diluted 1:500 in phosphate-buffered saline containing 0.1% (v/v) Triton X-100 (PBST). The sections were washed three times in PBST and then incubated for 2 h at 37°C with anti-rabbit IgG fluorescein-linked whole antibody from donkey (Amersham-Pharmacia) diluted 1:25 in PBST. After three washes in this buffer, the sections were mounted in antifading solution (FluoroGuard antifade reagent; Bio-Rad

Laboratories, Hercules, CA) and viewed under a confocal fluorescence microscope (Fluoview FV500 version 4.0; Olympus, Tokyo).

Microscopic Analysis

For light microscopy, tissues were fixed in FAA (5% formaldehyde, 5% glacial acetic acid, 63% ethanol) and dehydrated in a graded ethanol series. The samples were embedded in Paraplast Plus (Sherwood Medical, St. Louis). Microtome sections of 10 μm in thickness were applied to silane-coated glass slides (Matsunami Glass, Osaka). The sections were deparaffinized in xylene, dehydrated through a graded ethanol series, and dried overnight before staining with toluidine blue. To investigate the morphology of the epidermal cells of the leaf blade, the samples were cleared in benzyl-benzoate-four-and-a-half fluid (Herr, 1982).

Protein Extraction and Immunoblot Analysis

Proteins were extracted from seedlings by grinding in liquid nitrogen and resuspending the resulting powder in extraction buffer (20 mM Tris, pH 7.5, 150 mM NaCl, 0.5% Tween 20) containing 0.5 $\times$ Complete protease inhibitor solution (Roche, Mannheim, Germany). The extracts were cleared with two centrifugations of 20 min in a microcentrifuge. The protein concentrations of the soluble fractions were determined using Bradford reagent (Bio-Rad Laboratories) with bovine serum albumin as the standard. For immunoblot analysis, the proteins were separated by SDS-PAGE and transferred to Hybond ECL membrane (Amersham-Pharmacia Biotech, Uppsala) by semi-dry blotting. Immunoblot analysis was carried out with a 1:10,000 dilution of a rabbit anti-SLR1 serum (Itoh et al., 2002) as the primary antibody and a horseradish peroxidase-conjugated goat anti-rabbit IgG (Medical and Biological Laboratories, Nagoya, Japan) as the secondary antibody. Peroxidase activity was detected according to the method of the manufacturer (Pierce, Rockford, IL).

Reverse-Transcription Quantitative PCR

Wild-type and *dgl1* seeds were grown on 1% agar plates and sprayed with 10^{-4} M GA_3 or control solution as described above. Wild-type and *brd1-2* seeds were grown on 1% agar plates containing or lacking 10^{-6} M BL. Total RNAs were extracted as described above. First-strand cDNA was synthesized in a RT reaction with 2 μg of total RNA using the Omniscript reverse transcription kit (Qiagen). Quantitative PCR was performed using a Roche LightCycler (Roche) and the QuantiTect SYBR Green PCR kit, according to the manufacturer's instructions, at the appropriate annealing temperature for each gene (*OsGA20ox2/SD1*, 60°C; *OsGA20ox1*, 60°C; *OsGA3ox2/D18*, 72°C; *OsKAO*, 55°C; *OsCPD*, 55°C; *D11*, 57°C; *OsDWARF*, 57°C; and *ACTIN1*, 62°C). The 5′ and 3′ primers for each gene were as follows: *OsGA20ox2/SD1*, 5′-CAGCACTACCCGGACTTCAC-3′ and 5′-GCTTCTGTTCGTTCCGTTTC-3′; *OsGA20ox1*, 5′-TCGGCTGGAGATGAAGAGG-3′ and 5′-AAGAATCGCCGGAAGTAGTG-3′; *OsGA3ox2/D18*, 5′-TCTCCAAGCTCATGTGGTCCGAGGGCTA-3′ and 5′-TGGAGCACGAAGGTGAAGAAGCCCGAGT-3′; *OsKAO*, 5′-GAGATCGTCGACGTCCTCATCATGTACC-3′ and 5′-AGATGTTGACGCAGCGAAGTGTCTCGTC-3′; *OsCPD*, 5′-TTCTTCTCCATCCCCTTTCCTCTCGCCA-3′ and 5′-CACCCTCCGCCTCAAGAAGCTCCTCAA-3′; *D11*, 5′-TTGGGTCATGGCATGGCAAGAGCAAGGA-3′ and 5′-TTGTTGCTGGAGCCAGCATTCCTCCTCT-3′; *OsDWARF*, 5′-ATGGTGTTGGTGGCGATTGGGGTGGTTG-3′ and 5′-ATGTTGTTCCGCCCCAGGATGTCCAGCA-3′; and *ACTIN1*, 5′-CATCTTGGCATCTCTCAGCAC-3′ and 5′-AACTTTGTCCACGCTAATGAA-3′.

Received March 29, 2005; revised April 27, 2005; accepted May 1, 2005; published July 22, 2005.

LITERATURE CITED

Bichet A, Desnos T, Turner S, Grandjean O, Hofte H (2001) *BOTERO1* is required for normal orientation of cortical microtubules and anisotropic cell expansion in *Arabidopsis*. Plant J **25:** 137–148

Bouquin T, Mattsson O, Naested H, Foster R, Mundy J (2003) The *Arabidopsis lue1* mutant defines a katanin p60 ortholog involved in hormonal control of microtubule orientation during cell growth. J Cell Sci **116:** 791–801

Burk DH, Liu B, Zhong R, Morrison WH, Ye ZH (2001) A katanin-like protein regulates normal cell wall biosynthesis and cell elongation. Plant Cell **13:** 807–827

Burk DH, Ye ZH (2002) Alteration of oriented deposition of cellulose microfibrils by mutation of a katanin-like microtubule-severing protein. Plant Cell **14:** 2145–2160

Clouse SD, Sasse JM (1998) Brassinosteroids: essential regulators of plant growth and development. Annu Rev Plant Physiol Plant Mol Biol **49:** 427–451

Fleet CM, Sun TP (2005) A DELLAcate balance: the role of gibberellin in plant morphogenesis. Curr Opin Plant Biol **8:** 77–85

Foster R, Mattsson O, Mundy J (2003) Plants flex their skeletons. Trends Plant Sci **8:** 202–204

Fujioka S, Yokota T (2003) Biosynthesis and metabolism of brassinosteroids. Annu Rev Plant Biol **54:** 137–164

Gonzalez RG, Haxo RS, Schleich T (1980) Mechanism of action of polymeric aurintricarboxylic acid, a potent inhibitor of protein-nucleic acid interactions. Biochemistry **19:** 4299–4303

Hartman JJ, Mahr J, McNally K, Okawa K, Iwamatsu A, Thomas S, Cheesman S, Heuser J, Vale RD, McNally FJ (1998) Katanin, a microtubule-severing protein, is a novel AAA ATPase that targets to the centrosome using a WD40-containing subunit. Cell **93:** 277–287

Hartman JJ, Vale RD (1999) Microtubule disassembly by ATP-dependent oligomerization of the AAA enzyme katanin. Science **286:** 782–785

Herr JM Jr (1982) An analysis of methods for permanently mounting ovules cleared in four-and-a-half type clearing fluids. Stain Technol **57:** 161–169

Hiei Y, Ohta S, Komari T, Kumashiro T (1994) Efficient transformation of rice (*Oryza sativa* L.) mediated by *Agrobacterium* and sequence analysis of the boundaries of the T-DNA. Plant J **6:** 271–282

Hong Z, Ueguchi-Tanaka M, Matsuoka M (2004) Brassinosteroids and rice architecture. J Pestic Sci **29:** 184–188

Hong Z, Ueguchi-Tanaka M, Shimizu-Sato S, Inukai Y, Fujioka S, Shimada Y, Takatsuto S, Agetsuma M, Yoshida S, Watanabe Y, et al (2002) Loss-of-function of a rice brassinosteroid biosynthetic enzyme, C-6 oxidase, prevents the organized arrangement and polar elongation of cells in the leaves and stem. Plant J **32:** 495–508

Hood EE, Helmer GL, Fraley RT, Chilton MD (1986) The hypervirulence of *Agrobacterium tumefaciens* A281 is encoded in a region of pTiBo542 outside of T-DNA. J Bacteriol **168:** 1291–1301

Ikeda A, Ueguchi-Tanaka M, Sonoda Y, Kitano H, Koshioka M, Futsuhara Y, Matsuoka M, Yamaguchi J (2001) *slender* rice, a constitutive gibberellin response mutant, is caused by a null mutation of the *SLR1* gene, an ortholog of the height-regulating gene *GAI/RGA/RHT/D8*. Plant Cell **13:** 999–1010

Ishikawa S, Maekawa M, Arite T, Onishi K, Takamure I, Kyozuka J (2005) Suppression of tiller bud activity in tillering dwarf mutants of rice. Plant Cell Physiol **46:** 79–86

Itoh H, Tatsumi T, Sakamoto T, Otomo K, Toyomasu T, Kitano H, Ashikari M, Ichihara S, Matsuoka M (2004) A rice semi-dwarf gene, *Tan-Ginbozu* (*D35*), encodes the gibberellin biosynthesis enzyme, *ent*-kaurene oxidase. Plant Mol Biol **54:** 533–547

Itoh H, Ueguchi-Tanaka M, Sato Y, Ashikari M, Matsuoka M (2002) The gibberellin signaling pathway is regulated by the appearance and disappearance of SLENDER RICE1 in nuclei. Plant Cell **14:** 57–70

Itoh H, Ueguchi-Tanaka M, Sentoku N, Kitano H, Matsuoka M (2001) Cloning and functional analysis of two gibberellin 3β-hydroxylase genes that are differently expressed during the growth of rice. Proc Natl Acad Sci USA **98:** 8909–8914

Mandava NB (1988) Plant growth-promoting brassinosteroids. Annu Rev Plant Physiol Plant Mol Biol **39:** 23–52

Matsuo T, Futsuhara Y, Kikuchi F, Yamaguchi H (1997) Science of the Rice Plant, Vol 3. Nobunkyo, Tokyo, pp 302–303

McClinton RS, Chandler JS, Callis J (2001) cDNA isolation, characterization, and protein intracellular localization of a katanin-like p60 subunit from *Arabidopsis thaliana*. Protoplasma **216:** 181–190

McNally FJ, Okawa K, Iwamatsu A, Vale RD (1996) Katanin, the microtubule-severing ATPase, is concentrated at centrosomes. J Cell Sci **109:** 561–567

McNally FJ, Thomas S (1998) Katanin is responsible for the M-phase microtubule-severing activity in *Xenopus* eggs. Mol Biol Cell **9:** 1847–1861

McNally FJ, Vale RD (1993) Identification of katanin, an ATPase that severs and disassembles stable microtubules. Cell **75:** 419–429

McNally KP, Bazirgan OA, McNally FJ (2000) Two domains of p80 katanin regulate microtubule severing and spindle pole targeting by p60 katanin. J Cell Sci **113:** 1623–1633

Meier C, Bouquin T, Nielsen ME, Raventos D, Mattsson O, Rocher A, Schomburg F, Amasino RM, Mundy J (2001) Gibberellin response mutants identified by luciferase imaging. Plant J **25:** 509–519

Sakamoto T, Miura K, Itoh H, Tatsumi T, Ueguchi-Tanaka M, Ishiyama K, Kobayashi M, Agrawal GK, Takeda S, Abe K, et al (2004) An overview of gibberellin metabolism enzyme genes and their related mutants in rice. Plant Physiol **134:** 1642–1653

Sasaki A, Itoh H, Gomi K, Ueguchi-Tanaka M, Ishiyama K, Kobayashi M, Jeong DH, An G, Kitano H, Ashikari M, et al (2003) Accumulation of phosphorylated repressor for gibberellin signaling in an F-box mutant. Science **299:** 1896–1898

Stoppin-Mellet V, Gaillard J, Vantard M (2002) Functional evidence for *in vitro* microtubule severing by the plant katanin homologue. Biochem J **365:** 337–342

Taiz L, Zeiger E (2002) Plant Physiology, Ed 3. Sinauer Associates, Sunderland, MA, pp 461–488

Tanabe S, Ashikari M, Fujioka S, Takatsuto S, Yoshida S, Yano M, Yoshimura A, Kitano H, Matsuoka M, Fujisawa Y, et al (2005) A novel cytochrome P450 is implicated in brassinosteroid biosynthesis via the characterization of a rice dwarf mutant, *dwarf11*, with reduced seed length. Plant Cell **17:** 776–790

Vale RD (1991) Severing of stable microtubules by a mitotically activated protein in *Xenopus* egg extracts. Cell **64:** 827–839

Wasteneys GO (2002) Microtubule organization in the green kingdom: chaos or self-order? J Cell Sci **115:** 1345–1354

Webb M, Jouannic S, Foreman J, Linstead P, Dolan L (2002) Cell specification in the *Arabidopsis* root epidermis requires the activity of *ECTOPIC ROOT HAIR* 3-a katanin-p60 protein. Development **129:** 123–131

Yamamuro C, Ihara Y, Wu X, Noguchi T, Fujioka S, Takatsuto S, Ashikari M, Kitano H, Matsuoka M (2000) Loss of function of a rice *brassinosteroid insensitive1* homolog prevents internode elongation and bending of the lamina joint. Plant Cell **12:** 1591–1605